Quantum spectra of Raman photon pairs from a mesoscopic particle

C. H. Raymond Ooi,[1,2] W. M. Edmund Loh,[1] and C. H. Kam[2]
[1]*Department of Physics, University of Malaya, 50603 Kuala Lumpur, Malaysia*
[2]*School of Electrical and Electronic Engineering, Nanyang Technological University, Nanyang Avenue, 639798 Singapore*
(Received 13 February 2015; published 19 June 2015)

Quantum Langevin formalism with noise operators is used to provide quantum descriptions of photon pairs (the Stokes and anti-Stokes fields) emitted by a mesoscopic spherical particle composed of quantum particles in a double Raman configuration. The spectra of the fields obtained are sensitive to the dimension of the microsphere and can be controlled by pump and control laser fields. Spectral peaks due to quantum coherence are Stark shifted by the laser fields experiencing autofocusing inside the spherical particle, causing broadening of peaks as the size of the microsphere increases. The antinormal-order spectrum is found to be identical to the normal-order spectrum. The anti-Stokes spectrum is identical to the Stokes spectrum when the linear dispersion is neglected. Frequency-dependent dielectric functions of the Stokes and anti-Stokes spectra corresponding to the linear dispersions of the particle yield narrow morphology-dependent resonance gain peaks at certain frequencies of the Stokes and anti-Stokes spectra that depend not only on the particle size but also on the angle of observation.

DOI: 10.1103/PhysRevA.91.063826 PACS number(s): 42.50.Dv, 42.50.Gy, 42.50.Lc, 42.25.Fx

I. INTRODUCTION

Quantum properties of photon pairs in the double Raman scheme [1] have been studied in various systems such as single atoms [2], two atoms with dipole-dipole interaction [3], an array of atoms [4], a single-atom two-photon laser [5], and a one-dimensional amplifier [6]. These systems are relevant for generation of nonclassical photons in quantum information [7]. Recent progress in nanotechnology has stretched the applicability of quantum entanglement to nanophotonics [8]. The studies of quantum effects now extend to nanoparticles as well as microparticles [9].

Coherent Raman scattering of light by microparticles composed of atoms with quantum coherence has been studied using semiclassical theory [10] in the interest of enhancing backscattered signal. Also, optical bistability in a similar system has been investigated [11]. In particular, light scattered from spherical microparticles has prompted many theoretical studies that encompass areas such as stimulated emission processes [12], electronic Raman scattering [13], Raman coupling coefficients [14], and second-harmonic generation [15].

In this work we use quantum Langevin formalism [16] to describe the interactions of particles with pump and control laser fields inside a small spherical particle with arbitrary dimension (Fig. 1). This formalism correctly expresses the scattered Stokes and anti-Stokes electric fields as quantum operators in terms of the noise operators [17], which enables us to compute the quantum-mechanical expressions for field-field correlation functions in a transparent manner. In particular, we obtain the spectra [18] for both normal and antinormal-order expressions of the Stokes and anti-Stokes electric fields. The normal-order spectrum, being the Fourier transform of the first-order correlation function $G^{(1)}(\mathbf{r},t)$, plays an essential role in the description of the experimentally observed quantities such as photoelectron statistics.

The differences between the normal and antinormal-order correlations can be understood as follows. Normal-order correlation functions are utilized more frequently than the antinormal-order ones in the photodetection theory due to the ubiquity of the photon detection experiment based on the photoelectric effect [19]. However, there exists another possible photodetection method using the quantum counter introduced by Mandel [20], which can only be described by the antinormal-order correlation functions. Such a photon-counting device functions by stimulated emission rather than by absorption of photons and would be useful when the average number of photons is not too small. Thus, it is the creation operator instead of the annihilation operator that plays the central role. A comparison between the two distinct correlations is interesting in terms of the photodetected spectrum.

II. QUANTUM LANGEVIN FORMALISM FOR COHERENCES

The quantum Langevin formalism for quantum particles with the double Raman scheme in four levels a–d gives 16 coupled equations. If the Stokes $\hat{E}_s$ and anti-Stokes fields $\hat{E}_a$ are weak the populations and the coherences $\hat{\sigma}_{dc}$ and $\hat{\sigma}_{ab}$ can be approximated as complex numbers. This enables us to solve just the following four coupled equations

We have the closed coupled equations for the slowly varying atomic envelope operators of the coherences $\hat{p}_{ac} = \hat{\sigma}_{ac}e^{-i\nu_a t}$, $\hat{p}_{ad} = \hat{\sigma}_{ad}e^{-i\nu_{cs} t}$, $\hat{p}_{bc} = \hat{\sigma}_{bc}e^{-i\nu_{ac} t}$, and $\hat{p}_{bd} = \hat{\sigma}_{bd}e^{i\nu_s t}$, where $\nu_{ij} = \nu_i - \nu_j$ and ν_i $(i \in p,s,c,a)$ are the carrier frequencies of the pump, Stokes, control, and anti-Stokes fields, respectively, which satisfy $\nu_p + \nu_c = \nu_s + \nu_a$ for the closed (parametric four photons) transitions

$$\frac{d}{dt}\hat{p}_{ac} = -T_{ac}\hat{p}_{ac} - i\mathbf{g}_a^* \cdot \tilde{\mathbf{E}}_a^\dagger(\hat{p}_{cc} - \hat{p}_{aa}) - i(\Omega_c^*\hat{p}_{bc} - \Omega_p^*\hat{p}_{ad}) + e^{-i\nu_a t}\hat{F}_{ac}, \quad (1)$$

$$\frac{d}{dt}\hat{p}_{ad} = -T_{ad}\hat{p}_{ad} + i(\hat{p}_{ab}\mathbf{g}_s \cdot \tilde{\mathbf{E}}_s - \mathbf{g}_a^* \cdot \tilde{\mathbf{E}}_a^\dagger\hat{p}_{cd}) + i(\Omega_p\hat{p}_{ac} - \Omega_c^*\hat{p}_{bd}) + e^{-i\nu_{cs} t}\hat{F}_{ad}, \quad (2)$$

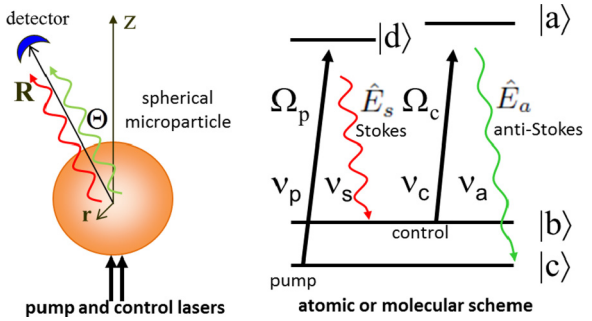

FIG. 1. (Color online) Illustration of a spherical particle composed of four-level atoms interacting with pump Ω_p and control Ω_p lasers (solid arrows) and emitting quantized Stokes $\hat{\mathbf{E}}_s$ and anti-Stokes $\hat{\mathbf{E}}_a$ fields (wavy arrows) with their respective frequencies ν_q $(q = p,s,c,a)$.

$$\frac{d}{dt}\hat{p}_{bc} = -T_{bc}\hat{p}_{bc} - i(\hat{p}_{dc}\mathbf{g}_s\cdot\tilde{\mathbf{E}}_s - \mathbf{g}_a^*\cdot\tilde{\mathbf{E}}_a^\dagger\hat{p}_{ba}) - i(\Omega_c\hat{p}_{ac} - \Omega_p^*\hat{p}_{bd}) + e^{i\nu_{ca}t}\hat{F}_{bc}, \tag{3}$$

$$\frac{d}{dt}\hat{p}_{bd} = -T_{db}^*\hat{p}_{bd} + i(\hat{p}_{bb} - \hat{p}_{dd})\mathbf{g}_s\cdot\tilde{\mathbf{E}}_s + i(\Omega_p\hat{p}_{bc} - \Omega_c\hat{p}_{ad}) + e^{i\nu_s t}\hat{F}_{db}^\dagger, \tag{4}$$

with $\hat{F}_{db}^\dagger = \hat{F}_{bd}$ and the complex decoherences

$$T_{ac} = i\Delta_a + \gamma_{ac}, \tag{5}$$

$$T_{ad} = i(\Delta_c - \Delta_s) + \gamma_{ad}, \tag{6}$$

$$T_{bc} = i(\Delta_p - \Delta_s) + \gamma_{bc}, \tag{7}$$

$$T_{db} = i\Delta_s + \gamma_{db}, \tag{8}$$

with the detunings $\Delta_p = \nu_p - \omega_{dc}$, $\Delta_s = \nu_s - \omega_{db}$, $\Delta_c = \nu_c - \omega_{ab}$, and $\Delta_a = \nu_a - \omega_{ac}$ of the pump, Stokes, control, and anti-Stokes fields, respectively. As before, the subscripts p, s, c, and a stand for pump, Stokes, control, and anti-Stokes fields, respectively. Also, ω_{ac} simply means the transition frequency between energy levels a and c and the same method of definition applies for the other cases. Here we may have the spatial dependence of the pump and control laser fields but neglect the temporal dependence, i.e., Ω_p and Ω_c are constant in time. Hence, the Rabi frequencies for the lasers $l = p,c$ are $\Omega_l(\mathbf{r}) = \mathbf{g}_l\cdot\tilde{\mathbf{E}}_l(\mathbf{r}) = \sum_{j=x,y,z} g_{lj}E_{lj}(\mathbf{r})$, where $g_{lj} = \wp_{lj}/\hbar$ with $\wp_{lj}$ as the jth component transition dipole moment. To solve for $\hat{p}_{ac}(\mathbf{r},\omega)$ and $\hat{p}_{bd}(\mathbf{r},\omega)$ we assume $\hat{p}_{aa} - \hat{p}_{cc} \approx w_{cc}^{st} = \langle\hat{p}_{aa} - \hat{p}_{cc}\rangle$, $\hat{p}_{dd} - \hat{p}_{bb} \approx w_{bb}^{st} = \langle\hat{p}_{dd} - \hat{p}_{bb}\rangle$, $\hat{p}_{ab} \approx \langle\hat{p}_{ab}^{st}\rangle = p_{ab}^{st}$, and $\hat{p}_{dc} \approx \langle\hat{p}_{dc}^{st}\rangle = p_{cd}^{st}$ to be the expectation values (the populations and the coherences at the laser transitions). After the Fourier transformation $F\{\cdots\} = \int_{-\infty}^{\infty}\{\cdots\}e^{i\omega t}dt$, the four coupled equations become

$$\hat{p}_{ac}(\mathbf{r},\omega) = \hat{\sigma}_{ac}(\omega - \nu_a) = \frac{1}{T_{ac}(\omega)}\left[i\tilde{A}^\dagger(\omega)w_{cc}^{st} - i\Omega_c^*\hat{p}_{bc}(\omega) + i\Omega_p^*\hat{p}_{ad}(\omega) + \hat{G}_{ac}(\omega)\right], \tag{9}$$

$$\hat{p}_{ad}(\mathbf{r},\omega) = \hat{\sigma}_{ad}(\omega - \nu_{cs}) = \frac{1}{T_{ad}(\omega)}\left[i\tilde{S}(\omega)p_{ab}^{st} - i\tilde{A}^\dagger(\omega)p_{cd}^{st} + i\Omega_p\hat{p}_{ac}(\omega) - i\Omega_c^*\hat{p}_{bd}(\omega) + \hat{G}_{ad}(\omega)\right], \tag{10}$$

$$\hat{p}_{bc}(\mathbf{r},\omega) = \hat{\sigma}_{bc}(\omega - \nu_{ac}) = \frac{1}{T_{bc}(\omega)}\left[-i\tilde{S}(\omega)p_{dc}^{st} + i\tilde{A}^\dagger(\omega)p_{ba}^{st} - i\Omega_c\hat{p}_{ac}(\omega) + i\Omega_p^*\hat{p}_{bd}(\omega) + \hat{G}_{bc}(\omega)\right], \tag{11}$$

$$\hat{p}_{bd}(\mathbf{r},\omega) = \hat{\sigma}_{bd}(\omega + \nu_s) = \frac{1}{T_{db}^*(\omega)}\left[-i\tilde{S}(\omega)w_{bb}^{st} + i\Omega_p\hat{p}_{bc}(\omega) - i\Omega_c\hat{p}_{ad}(\omega) + \hat{G}_{bd}(\omega)\right], \tag{12}$$

where

$$\tilde{Q}(\mathbf{r},\omega) = \int_{-\infty}^{\infty}\tilde{Q}(\mathbf{r},t)e^{i\omega t}dt = \int_{-\infty}^{\infty}\hat{O}(\mathbf{r},t)e^{i\omega t}e^{-i\nu_x t}dt = \hat{O}(\mathbf{r},\omega - \nu_x),$$

with $\tilde{Q} \in \tilde{E}_s,\tilde{E}_a^\dagger,\hat{p}_x,\hat{G}_x$ $(x \in ac,ad,bc,bd)$ the Fourier transforms of the original operators $\hat{O} \in \hat{E}_s,\hat{E}_a^\dagger,\hat{\sigma}_x,\hat{F}_x$ with the rapidly varying phases $\nu_x t$. Therefore, the conjugates are $\hat{Q}^\dagger(\mathbf{r},\omega) = \hat{O}^\dagger[\mathbf{r},-(\omega - \nu_x)]$. We define $\tilde{S} = \mathbf{g}_s\cdot\tilde{\mathbf{E}}_s = \sum_{j=x,y,z} g_{sj}\tilde{E}_{sj}$ and $\tilde{A} = \mathbf{g}_a\cdot\tilde{\mathbf{E}}_a = \sum_{j=x,y,z} g_{aj}\tilde{E}_{aj}$, with $g_{sj} = \frac{1}{\hbar}\wp_{db,j}$ and $g_{aj} = \frac{1}{\hbar}\wp_{ac,j}$, and the complex decoherences after Fourier transformation are $T_x(\omega) = T_x - i\omega$ and $T_{db}^*(\omega) = T_{db}^* - i\omega$.

Thus we have the solutions

$$\begin{pmatrix}\hat{p}_{ac}\\ \hat{p}_{ad}\\ \hat{p}_{bc}\\ \hat{p}_{bd}\end{pmatrix} = -\begin{pmatrix}-T_{ac}(\omega) & i\Omega_p^* & -i\Omega_c^* & 0\\ i\Omega_p & -T_{ad}(\omega) & 0 & -i\Omega_c^*\\ -i\Omega_c & 0 & -T_{bc}(\omega) & i\Omega_p^*\\ 0 & -i\Omega_c & i\Omega_p & -T_{db}^*(\omega)\end{pmatrix}^{-1}\begin{pmatrix}i\hat{A}^\dagger w_{cc}^{st} + \hat{G}_{ac}\\ i\hat{S}p_{ab}^{st} - i\hat{A}^\dagger p_{cd}^{st} + \hat{G}_{ad}\\ -i\hat{S}p_{dc}^{st} + i\hat{A}^\dagger p_{ba}^{st} + \hat{G}_{bc}\\ -i\hat{S}w_{bb}^{st} + \hat{G}_{bd}\end{pmatrix}. \tag{13}$$

At this point, we note that the pump and control laser fields inside the microparticle depend on the spatial coordinates of the particle. This is due to refraction and focusing by the geometry of the particle and it is taken into account by the Lorentz-Mie theory [10,21], assuming that the incident laser fields are x polarized. In particular, the coherences associated

with the Stokes and anti-Stokes fields are, respectively,

$$\hat{p}_{bd}(\mathbf{r},\omega) = -\left(\sum_{j=1}^{4} M_{4j}\hat{G}_j + X_s\hat{A}^\dagger + G_s\tilde{S}\right), \quad (14)$$

$$\hat{p}_{ac}(\mathbf{r},\omega) = -\left(\sum_{j=1}^{4} M_{1j}\hat{G}_j + G_a\hat{A}^\dagger + X_a\tilde{S}\right), \quad (15)$$

with the coefficients

$$G_s = i\left(p^{st}_{ab}M_{42} - p^{st}_{dc}M_{43} - w^{st}_{bb}M_{44}\right), \quad (16)$$

$$G_a = i\left(w^{st}_{cc}M_{11} - p^{st}_{cd}M_{12} + p^{st}_{ba}M_{13}\right), \quad (17)$$

$$X_s = i\left(w^{st}_{cc}M_{41} - p^{st}_{cd}M_{42} + p^{st}_{ba}M_{43}\right), \quad (18)$$

$$X_a = i\left(p^{st}_{ab}M_{12} - p^{st}_{dc}M_{13} - w^{st}_{bb}M_{14}\right), \quad (19)$$

where $\hat{G}_1 = \hat{G}_{ac}$, $\hat{G}_2 = \hat{G}_{ad}$, $\hat{G}_3 = \hat{G}_{bc}$, $\hat{G}_4 = \hat{G}_{bd}$, and M is the inverse of the 4×4 matrix in Eq. (13) above that can be obtained analytically.

III. STOKES AND ANTI-STOKES ELECTRIC FIELDS

We now couple the quantum coherence operators of the quantum particles to the electric-field operators of the Stokes and anti-Stokes quantum fields $\hat{\mathbf{E}}_f$ ($f \in s,a$)

$$\left(\nabla^2 + \frac{\omega^2}{c^2}\right)\hat{\mathbf{E}}_f(\mathbf{r},\omega) = -\frac{1}{\varepsilon_o}\left\{\nabla\nabla\cdot + \frac{\omega^2}{c^2}\right\}\hat{\mathbf{P}}_f(\mathbf{r},\omega) \quad (20)$$

using the quantum-mechanical expression of the nonlinear polarization $\hat{\mathbf{P}}_f(\mathbf{r},\omega) = N\vec{\wp}_f\hat{\sigma}_f(\mathbf{r},\omega)$, where $N \simeq 10^{27}$ m^{-3} is the number density, $\vec{\wp}_s = \vec{\wp}_{bd} = \langle b|\mathbf{d}|d\rangle$ and $\vec{\wp}_a = \vec{\wp}_{ca} = \langle c|\mathbf{d}|a\rangle$ are the dipole matrix elements, and $\hat{\sigma}_s = \hat{\sigma}_{bd} = |b\rangle\langle d|$ and $\hat{\sigma}_a = \hat{\sigma}_{ca} = |c\rangle\langle a|$ are the coherence operators corresponding to the Stokes and anti-Stokes transitions, respectively. The far-field solution of a mesoscopic particle (assumed to be spherical) is

$$\hat{\mathbf{E}}_f(\mathbf{R},\omega) = \frac{\omega^2}{c^2}\int_V \frac{\left\{\hat{\Theta}\hat{P}^{NL}_{\Theta,f} + \hat{\Phi}\hat{P}^{NL}_{\Phi,f}\right\}e^{ik_f(\omega)|\mathbf{R}-\mathbf{r}|}}{4\pi\varepsilon_o|\mathbf{R}-\mathbf{r}|}d^3r, \quad (21)$$

where the dispersive wave vector $k_f(\omega)$ is related to the dielectric function $\varepsilon_f(\omega)$ by $k_f(\omega) = \sqrt{\varepsilon_f(\omega)}\omega/c$. The observation point is at $\mathbf{R} = R(\sin\Theta\cos\Phi, \sin\Theta\sin\Phi, \cos\Theta)$ and the position of a dipole is $\mathbf{r} = r(\sin\theta\cos\phi, \sin\theta\sin\phi, \cos\theta)$. The distance is $|\mathbf{R}-\mathbf{r}| = \sqrt{\Delta_x^2+\Delta_y^2+\Delta_z^2}$, where $\Delta_x = X - x$, etc. The $\hat{P}^{NL}_{\Theta,f}$ and $\hat{P}^{NL}_{\Phi,f}$ are the Θ and Φ components of the nonlinear polarization $\hat{\mathbf{P}}^{NL}_f$ and can be written as $\hat{P}^{NL}_{\Theta,f} = \hat{\Theta}\cdot\hat{\mathbf{P}}^{NL}_f$ and $\hat{P}^{NL}_{\Phi,f} = \hat{\Phi}\cdot\hat{\mathbf{P}}^{NL}_f$, respectively. Given the transformation unit vectors $\hat{\Theta} = (\cos\Theta\cos\Phi, \cos\Theta\sin\Phi, -\sin\Theta)$ and $\hat{\Phi} = (-\sin\Phi, \cos\Phi, 0)$, the electric-field vector can be decomposed into the Cartesian components $\hat{\mathbf{E}}_f = [\hat{E}_{fx}, \hat{E}_{fy}, \hat{E}_{fz}]$. To couple the Stokes and anti-Stokes quantum fields to the atomic operators, Eq. (21) is written as

$$\begin{pmatrix}\hat{\mathbf{E}}_s(\omega)\\ \hat{\mathbf{E}}^\dagger_a(\omega)\end{pmatrix} = \int_V \begin{pmatrix}K_s(\mathbf{r},\omega)\vec{\wp}^\perp_{bd}\hat{\sigma}^{NL}_{bd}(\mathbf{r},\omega)\\ K^*_a(\mathbf{r},\omega)\vec{\wp}^\perp_{ac}\hat{\sigma}^{NL}_{ac}(\mathbf{r},\omega)\end{pmatrix}d^3r, \quad (22)$$

where $K_f(\mathbf{r},\omega) = \frac{\omega^2}{c^2}\frac{N}{4\pi\varepsilon_o|\mathbf{R}-\mathbf{r}|}e^{ik_f(\omega)|\mathbf{R}-\mathbf{r}|}$ with the dispersive wave vector $k_f(\omega) = \sqrt{\varepsilon_f(\omega)}\omega/c$ and $\varepsilon_f(\omega)$ the dielectric function. The transverse dipole moment vector is

$$\vec{\wp}^\perp_g = \hat{\Theta}\wp_{\Theta,g} + \hat{\Phi}\wp_{\Phi,g} \quad (23)$$

with the angular components $\wp_{\Theta,g} = \hat{\Theta}\cdot\vec{\wp}_g, \wp_{\Phi,g} = \hat{\Phi}\cdot\vec{\wp}_g$ where $g \in bd, ac$.

Noting that the slowly varying envelope of the field is defined by $\hat{E}_{fq}(\mathbf{R},t) = \tilde{E}_{fq}(\mathbf{R},t)e^{-i\nu_f t}$ ($q \in x,y,z$), the Fourier transforms of the envelope operators are related as

$$\begin{pmatrix}\hat{\sigma}_{bd}(\omega)\\ \hat{\mathbf{E}}_s(\omega)\end{pmatrix} = \int e^{i(\omega-\nu_s)t}\begin{pmatrix}\hat{p}_{bd}(t)\\ \tilde{\mathbf{E}}_s(t)\end{pmatrix}dt = \begin{pmatrix}\hat{p}_{bd}(\omega_s^-)\\ \tilde{\mathbf{E}}_s(\omega_s^-)\end{pmatrix}, \quad (24)$$

$$\begin{pmatrix}\hat{\sigma}_{ac}(\omega)\\ \hat{\mathbf{E}}^\dagger_a(\omega)\end{pmatrix} = \int e^{i(\omega+\nu_a)t}\begin{pmatrix}\hat{p}_{ac}(t)\\ \tilde{\mathbf{E}}^\dagger_a(t)\end{pmatrix}dt = \begin{pmatrix}\hat{p}_{ac}(\omega_a^+)\\ \tilde{\mathbf{E}}^\dagger_a(\omega_a^+)\end{pmatrix}, \quad (25)$$

where $\omega - \nu_s = \omega_s^-$ and $\omega + \nu_a = \omega_a^+$ give $\tilde{\mathbf{E}}_s(\omega) = \hat{\mathbf{E}}_s(\omega + \nu_s)$ and $\tilde{\mathbf{E}}^\dagger_a(\omega) = \hat{\mathbf{E}}^\dagger_a(\omega - \nu_a)$. Hence, the quantum fields become

$$\begin{pmatrix}\hat{\mathbf{E}}_s(\omega)\\ \hat{\mathbf{E}}^\dagger_a(\omega)\end{pmatrix} = \int_V \begin{pmatrix}K_s(\mathbf{r},\omega)\vec{\wp}^\perp_{bd}\hat{p}^{NL}_{bd}(\mathbf{r},\omega_s^-)\\ K^*_a(\mathbf{r},\omega)\vec{\wp}^\perp_{ac}\hat{p}^{NL}_{ac}(\mathbf{r},\omega_a^+)\end{pmatrix}d^3r. \quad (26)$$

However, we have to compute $\hat{p}^{NL}_{bd}(\mathbf{r},\omega)$ and $\hat{p}^{NL}_{ac}(\mathbf{r},\omega)$, which are the solutions of the coupled equations [instead of $\hat{p}^{NL}_{bd}(\mathbf{r},\omega_s^-)$ and $\hat{p}^{NL}_{ac}(\mathbf{r},\omega_a^+)$], which give the Fourier transforms of the envelope field operators

$$\begin{pmatrix}\tilde{\mathbf{E}}_s(\omega)\\ \tilde{\mathbf{E}}^\dagger_a(\omega)\end{pmatrix} = N\int_V \begin{pmatrix}C_s(\mathbf{r},\omega)\vec{\wp}^\perp_{bd}\hat{p}^{NL}_{bd}(\mathbf{r},\omega)\\ C^*_a(\mathbf{r},\omega)\vec{\wp}^\perp_{ac}\hat{p}^{NL}_{ac}(\mathbf{r},\omega)\end{pmatrix}d^3r, \quad (27)$$

where $C_s(\mathbf{r},\omega) = \frac{(\omega+\nu_s)^2}{c^2}\frac{e^{ik_s(\omega+\nu_s)|\mathbf{R}-\mathbf{r}|}}{4\pi\varepsilon_o|\mathbf{R}-\mathbf{r}|}$ and $C_a(\mathbf{r},\omega) = \frac{(\omega-\nu_a)^2}{c^2}\frac{e^{ik_a(\omega-\nu_a)|\mathbf{R}-\mathbf{r}|}}{4\pi\varepsilon_o|\mathbf{R}-\mathbf{r}|}$. The wave vectors that include linear dispersion in the dielectric functions are $k_s(\omega+\nu_s) = \sqrt{\varepsilon_s(\mathbf{r},\omega+\nu_s)}(\omega+\nu_s)/c$ and $k_a(\omega-\nu_a) = \sqrt{\varepsilon_s(\mathbf{r},\omega-\nu_a)}(\omega-\nu_a)/c$ with the dispersive dielectric functions

$$\begin{pmatrix}\varepsilon_s(\mathbf{r},\omega+\nu_s)\\ \varepsilon^*_a(\mathbf{r},\omega-\nu_a)\end{pmatrix} = 1 + \frac{N}{\hbar\varepsilon_o}\begin{pmatrix}G_s(\mathbf{r},\omega)|\wp_{db}|^2\\ G_a(\mathbf{r},\omega)|\wp_{ca}|^2\end{pmatrix}. \quad (28)$$

The superscript NL excludes the term proportional to the respective quantum fields, thus

$$\hat{p}^{NL}_{bd}(\omega) = -\left(\sum_{j=1}^{4} M_{4j}\hat{G}_j + X_s\hat{A}^\dagger\right),$$
$$\hat{p}^{NL}_{ac}(\omega) = -\left(\sum_{j=1}^{4} M_{1j}\hat{G}_j + X_a\hat{S}\right). \quad (29)$$

.

IV. STOKES SPECTRUM

From the electric-field operators we obtain the power spectrum (from Appendix A) for the Stokes and anti-Stokes signals after applying the diffusion coefficients obtained from the noise correlations in Appendix B and the solutions of the matrix elements given in Appendix C.

A. Normal-order Stokes spectrum

For weak fields, only the first terms in Eqs. (14) and (15) are significant. The electric-field vector of the Stokes signal follows from Eq. (27),

$$\tilde{\mathbf{E}}_s(\omega) = -N\vec{\wp}_{bd}^{\perp}\int_V C_s(\mathbf{r},\omega)\sum_{j=1}^{4} M_{4j}(\mathbf{r},\omega)\hat{G}_j(\mathbf{r},\omega)d^3r. \tag{30}$$

Consider first the q component of the electric field. The normal-order correlation is

$$\begin{aligned}\langle\tilde{E}_{sq}^{\dagger}(-\omega')\tilde{E}_{sq}(\omega)\rangle &= N^2|\wp_{bd,q}^{\perp}|^2\int_V [C_s(\mathbf{r}',\omega')]^* C_s(\mathbf{r},\omega)\\ &\times\sum_{,j,l=1}^{4}[M_{4j}(\mathbf{r}',\omega')]^* M_{4l}(\mathbf{r},\omega)\\ &\times\langle[\hat{G}_j(\mathbf{r}',\omega')]^{\dagger}\hat{G}_l(\mathbf{r},\omega)\rangle d^3r'd^3r.\end{aligned} \tag{31}$$

From [6], the normal-order noise correlation products in the frequency domain are

$$\begin{aligned}\langle[\hat{G}_j(\mathbf{r}',\omega')]^{\dagger}\hat{G}_l(\mathbf{r},\omega)\rangle &= \langle\hat{G}_{j\dagger}(\mathbf{r}',-\omega')\hat{G}_l(\mathbf{r},\omega)\rangle\\ &= \frac{(2\pi)^3}{N}2\tilde{D}_{j\dagger,l}(\mathbf{r},\omega'-\omega)\delta(\mathbf{r}'-\mathbf{r})\\ &= \frac{(2\pi)^3}{N}2\tilde{D}_{j,l}^{n}(\mathbf{r},\omega'-\omega)\delta(\mathbf{r}'-\mathbf{r}),\end{aligned} \tag{32}$$

where the diffusion coefficient in the frequency domain $2\tilde{D}_{j,l}^{n}(w) = \int e^{iwt}2\tilde{D}_{j\dagger,l}(t)dt$ is related to that in time domain $\tilde{D}_{j\dagger,l}(t) = e^{i(\nu_j-\nu_l)t}D_{j\dagger,l}(t)$ as defined in Appendix B, while $j,l\in\{ac,ad,bc,bd\}$ and $j^*,l^*\in\{ca,da,cb,db\}$. We have used $\langle F_j^{\dagger}(\mathbf{r}',t')F_l(\mathbf{r},t)\rangle = 2D_{j\dagger,l}(\mathbf{r}',t')\delta(t-t')\frac{(2\pi)^3}{N}\delta(\mathbf{r}'-\mathbf{r})$ and evaluated $\langle[\hat{G}_j(\mathbf{r}',\omega')]^{\dagger}\hat{G}_l(\mathbf{r},\omega)\rangle$ through the steps

$$\begin{aligned}&\left\langle\int e^{-i\omega't'}e^{i\nu_j t'}F_j^{\dagger}(\mathbf{r}',t')dt'\int e^{i\omega t}e^{-i\nu_l t}F_l(\mathbf{r},t)dt\right\rangle\\ &= \int e^{-i\omega't'}dt'\int e^{i\omega t}dt e^{i\nu_j t'}e^{-i\nu_l t}\langle F_j^{\dagger}(\mathbf{r}',t')F_l(\mathbf{r},t)\rangle\\ &= \int e^{i(\omega-\omega'+\nu_j-\nu_l)t}2D_{j\dagger,l}(\mathbf{r}',t)dt\frac{(2\pi)^3}{N}\delta(\mathbf{r}'-\mathbf{r}).\end{aligned} \tag{33}$$

In spherical polar coordinates $d^3r = r^2\sin\theta d\theta d\phi dr$. In the far field

$$\begin{aligned}|\mathbf{R}-\mathbf{r}| &\approx R-\hat{R}\cdot\mathbf{r} = R-\frac{\mathbf{R}}{R}\cdot\mathbf{r}\\ &= R-r[\sin\Theta\sin\theta\cos(\Phi-\phi)+\cos\Theta\cos\theta].\end{aligned} \tag{34}$$

Since

$$\begin{aligned}R^2 \gg |&-2Rr[\sin\Theta\sin\theta\cos(\Phi-\phi)+\cos\Theta\cos\theta]\\ &+r^2[\sin\Theta\sin\theta\cos(\Phi-\phi)+\cos\Theta\cos\theta]^2|\end{aligned}$$

in the denominator we have $|\mathbf{R}-\mathbf{r}|^2\approx R^2$. From Eqs. (A1), (31), and (32) we have the Stokes spectrum

$$\begin{aligned}S_{sq}^{n}(\omega) &= \mathrm{Re}\langle\tilde{E}_{sq}^{\dagger}(\omega')\tilde{E}_{sq}(\omega)\rangle,\\ S_{sq}^{n}(\omega) &= AN|\wp_{sq}^{\perp}|^2(\omega+\nu_s)^4\\ &\times\sum_{j,l=1}^{4}\int_{r=0}^{\rho}\int_{\theta=0}^{\pi}\int_{\phi=0}^{2\pi}e^{2\,\mathrm{Im}k_s(\omega+\nu_s)\hat{R}\cdot\mathbf{r}}\\ &\times M_{4j}^{*}(\mathbf{r},\omega)M_{4l}(\mathbf{r},\omega)2\tilde{D}_{j,l}^{n}(\mathbf{r},0)d^3r,\end{aligned} \tag{35}$$

where $A = (\frac{1}{4\pi\varepsilon_o c^2 R})^2(2\pi)^3$, $d^3r = r^2\sin\theta d\theta d\phi dr$, and ρ is the radius of the spherical particle. Note that the spectrum is independent of the observation angles Θ and Φ since angular dependence is entirely in the term $\wp_{sq}^{\perp *}\wp_{sq}^{\perp}$ that is uncorrelated to any frequency-dependent term.

If the laser fields are homogeneous across the microparticle, the M matrix elements would be independent of position, hence the spectra would be essentially the same as a single atom. The second line becomes $\sum_{,j,l=1}^{4}M_{4j}^{*}M_{4l}\tilde{D}_{j,l}^{n}$. Thus, in the far-field approximation and assuming homogeneous excitations,

$$\begin{aligned}S_{sq}^{n}(\omega) &= AN|\wp_{bd,q}^{\perp}|^2\frac{4\pi}{3}\rho^3(\omega+\nu_s)^4\\ &\times\sum_{j,l=1}^{4}M_{4j}^{*}(\omega)M_{4l}(\omega)2\tilde{D}_{j,l}^{n}(0).\end{aligned} \tag{36}$$

B. Antinormal-order Stokes spectrum

To obtain the antinormal-order field correlation, we use the antinormal-order noise correlation

$$\langle\hat{G}_j(\mathbf{r}',\omega')\hat{G}_l^{\dagger}(\mathbf{r},\omega)\rangle = \frac{(2\pi)^3}{N}2\tilde{D}_{j,l}^{an}(\omega'-\omega)\delta(\mathbf{r}'-\mathbf{r}). \tag{37}$$

The q component of the electric-field correlation is the same as above except the diffusion coefficient $\tilde{D}_{j,l}^{n}$ is replaced by $\tilde{D}_{j,l}^{an}$. Similarly, the antinormal-order power spectrum $S_{sq}^{an}(\omega) = \mathrm{Re}\langle\tilde{E}_{sq}(\omega)\tilde{E}_{sq}^{\dagger}(\omega)\rangle$ due to the q component of the Stokes signal is

$$\begin{aligned}S_{sq}^{an}(\omega) &= AN|\wp_{bd,q}^{\perp}|^2(\omega+\nu_s)^4\sum_{j,l=1}^{4}\int_V e^{2\,\mathrm{Im}k_s(\omega+\nu_s)\hat{R}\cdot\mathbf{r}}\\ &\times M_{4j}(\mathbf{r},\omega)M_{4l}^{*}(\mathbf{r},\omega)2\tilde{D}_{j,l}^{an}(\mathbf{r},0)d^3r.\end{aligned} \tag{38}$$

V. ANTI-STOKES SPECTRUM

The electric-field vector of the anti-Stokes signal is given by

$$\tilde{\mathbf{E}}_a^{\dagger}(\omega) = -N\vec{\wp}_{ac}^{\perp}\int_V C_a(\mathbf{r},\omega)\sum_{j=1}^{4}M_{1j}(\mathbf{r},\omega)\hat{G}_j(\mathbf{r},\omega)d^3r. \tag{39}$$

The q component of normal-order power spectrum of the anti-Stokes signal is

$$\begin{aligned}S_{aq}^{n}(\omega) &= AN|\wp_{ac,q}^{\perp}|^2(\omega-\nu_a)^4\sum_{j,l=1}^{4}\int_V e^{2\,\mathrm{Im}k_a(\omega-\nu_a)\hat{R}\cdot\mathbf{r}}\\ &\times M_{1j}(\mathbf{r},\omega)M_{1l}^{*}(\mathbf{r},\omega)2\tilde{D}_{j,l}^{an}(\mathbf{r},0)d^3r.\end{aligned} \tag{40}$$

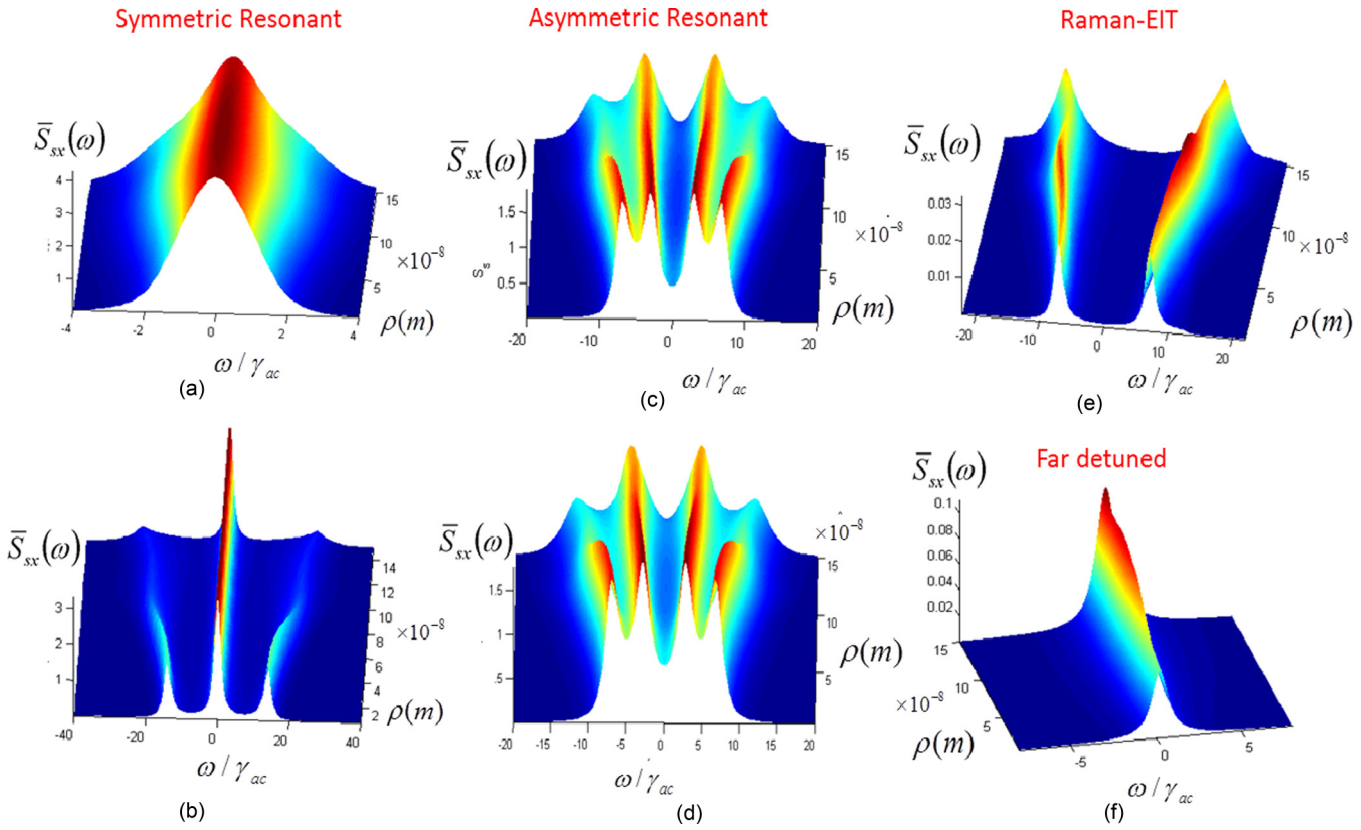

FIG. 2. (Color online) The x-component spectra of the Stokes spectra (same as the anti-Stokes spectra) versus particle radii ρ *without* linear dispersion for cases of resonant ($\Delta_p = \Delta_s = \Delta_c = \Delta_a = 0$) and symmetric laser fields (a) $\Omega_p = \Omega_c = \gamma_{ac}$ and (b) $\Omega_p = \Omega_c = 10\gamma_{ac}$; resonant and asymmetric laser fields (c) $\Omega_p = 3\gamma_{ac}$ and $\Omega_c = 7\gamma_{ac}$ and (d) $\Omega_p = 7\gamma_{ac}$ and $\Omega_c = 3\gamma_{ac}$; (e) Raman-EIT $\Delta_p = \Delta_s = -20\gamma_{ac}$, $\Delta_c = \Delta_a = 0$, $\Omega_p = 1\gamma_{ac}$, and $\Omega_c = 10\gamma_{ac}$; and (f) off-resonance configurations $\Delta_p = \Delta_s = \Delta_c = \Delta_a = -20\gamma_{ac}$, $\Omega_p = \gamma_{ac}$, and $\Omega_c = 3\gamma_{ac}$. Other parameters used (defined in Appendix C) are $\Gamma_x = \Gamma = 5 \times 10^7\ \mathrm{s}^{-1}$ with $x = ac,ab,db,dc$; $\bar{n}_x = [\exp(\theta_x) - 1]^{-1}$; and $\theta_x = \hbar\omega_x/k_BT$ at temperature $T = 300$ K.

The q-component antinormal-order power spectrum of the anti-Stokes signal

$$S^{an}_{aq}(\omega) = AN|\wp^{\perp}_{ac,q}|^2(\omega - \nu_a)^4 \sum_{j,l=1}^{4} \int_V e^{2\,\mathrm{Im}k_a(\omega-\nu_a)\hat{R}\cdot\mathbf{r}} \times M^*_{1j}(\mathbf{r},\omega)M_{1l}(\mathbf{r},\omega)2\tilde{D}^n_{j,l}(\mathbf{r},0)d^3r. \quad (41)$$

We note that the anti-Stokes spectrum would be identical to the Stokes spectrum, not only when the pump and control laser parameters are the same, i.e., $\Omega_p = \Omega_c$, but for any parameters, due to symmetry from the small separation between levels b and c. Also, the spectra would not depend on the dispersion of the wave vector if the dielectric functions $\varepsilon_s(\omega)$ and $\varepsilon_a(\omega)$ were real. The imaginary part would be responsible for the damping (or amplification) of the fields inside the particle, as well as the directional dependence [22] of the spectra.

VI. RESULTS AND DISCUSSION

The Stokes and anti-Stokes spectra are plotted in Figs. 2–7, showing the change in the spectra with particle radius ρ for four cases of laser parameters at resonance: (i) small and same laser strengths $\Omega_p = \Omega_c = \gamma_{ac}$, (ii) large and same laser strengths $\Omega_p = \Omega_c = 10\gamma_{ac}$, (iii) different laser strengths $\Omega_p = 3\gamma_{ac}$ and $\Omega_c = 7\gamma_{ac}$, and (iv) the opposite $\Omega_p = 7\gamma_{ac}$ and Ω_c=$3\gamma_{ac}$.

The dimensionless spectrum (noted with an overbar)

$$\bar{S}_{s(a)q}(\omega) = S_{s(a)q}(\omega)\frac{\Gamma_{db(ac)}}{ANV|\wp_{db(ac)}|^2\nu^4_{s(a)}} \quad (42)$$

for the Stokes s or anti-Stokes a fields with the component q (for x,y,z) is plotted by multiplying $S^n_{fq}(\omega)$ by a factor shown above with $V = \frac{4\pi}{3}\rho^3$. The focusing effect of the spherical particle gives rise to spatially inhomogeneous pump and control fields inside the particle. This effect is included using the Mie theory (see the Appendix of Ref. [15]) with refractive indices $n_p = 1.5$ and $n_c = 1.4$.

Resonant peaks. When both pump and control laser fields have the same value, the triple (Mollow) peaks [Fig. 2(b)] are clearly visible for the small-particle case (which describes well the single-atom scenario) and their separation increases with higher laser fields. When the fields have different values $\Omega_p \neq \Omega_c$, there are four strong resonant peaks at $-(\Omega_p + \Omega_c)$, $-|\Omega_p - \Omega_c|$, $|\Omega_p - \Omega_c|$, and $\Omega_p + \Omega_c$, which can all be explained as due to Autler-Townes splittings.

Normal vs antinormal order. The antinormal order corresponds to the opposite process, i.e., stimulated emission instead of absorption [20]. Mathematically, the difference between Eqs. (35) and (40) and Eqs. (38) and (41) is in the diffusion coefficients, but the coefficients are frequency independent. For the small-particle regime, any differences

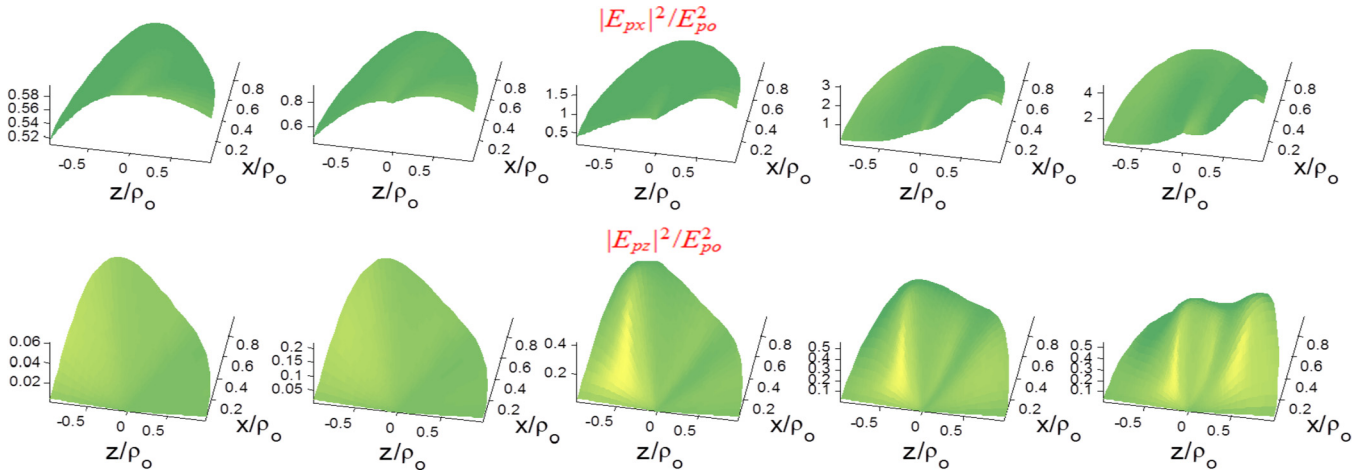

FIG. 3. (Color online) Normalized field intensity distributions $|E_{px}|^2/E_{po}^2$ and $|E_{pz}|^2/E_{po}^2$ for the pump laser for the five different radii ρ. Note that $|E_{pz}|^2$ is smaller than $|E_{px}|^2$.

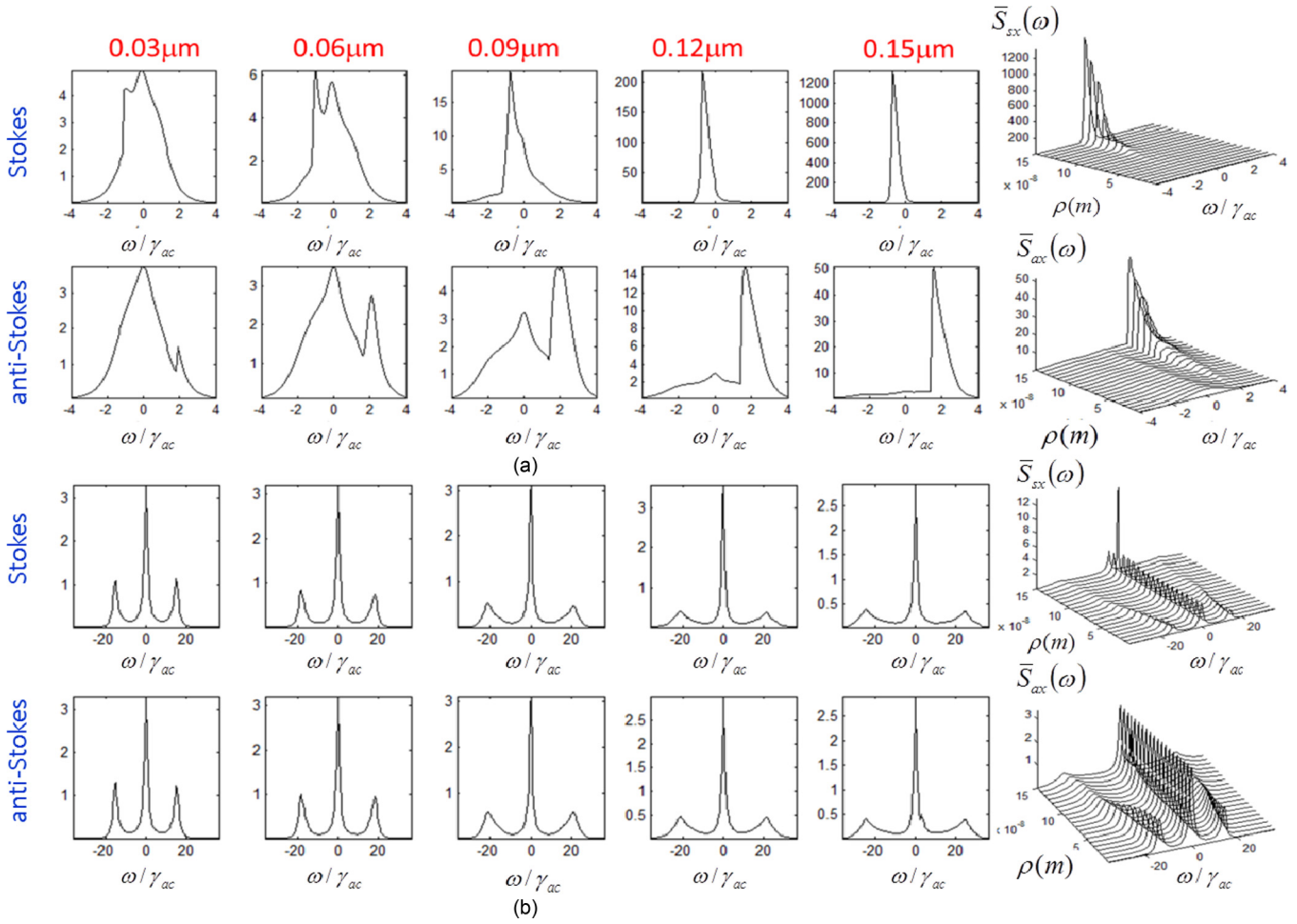

FIG. 4. (Color online) Normal-order x component of Stokes spectra (upper panels) and anti-Stokes spectra (lower panels) with linear dispersion for particle radii ρ arranged in increasing size. The lasers are resonant and equal strength (symmetric resonant) for (a) weak fields $\Omega_p = \Omega_c = \gamma_{ac}$ and (b) strong fields $\Omega_p = \Omega_c = 10\gamma_{ac}$. The observation direction is $\Theta = \Phi = 0$. Other parameters used are $\Delta_x = 0$, $\Gamma_x = \Gamma(\bar{n}_x + 1)$, and $\Gamma = 5 \times 10^7 \mathrm{s}^{-1}$ with $x = ac,ab,db,dc$; $\bar{n}_x = (e^{\theta_x} - 1)^{-1}$; $\theta_x = \hbar\omega_x/k_B T$; and $T = 300$ K.

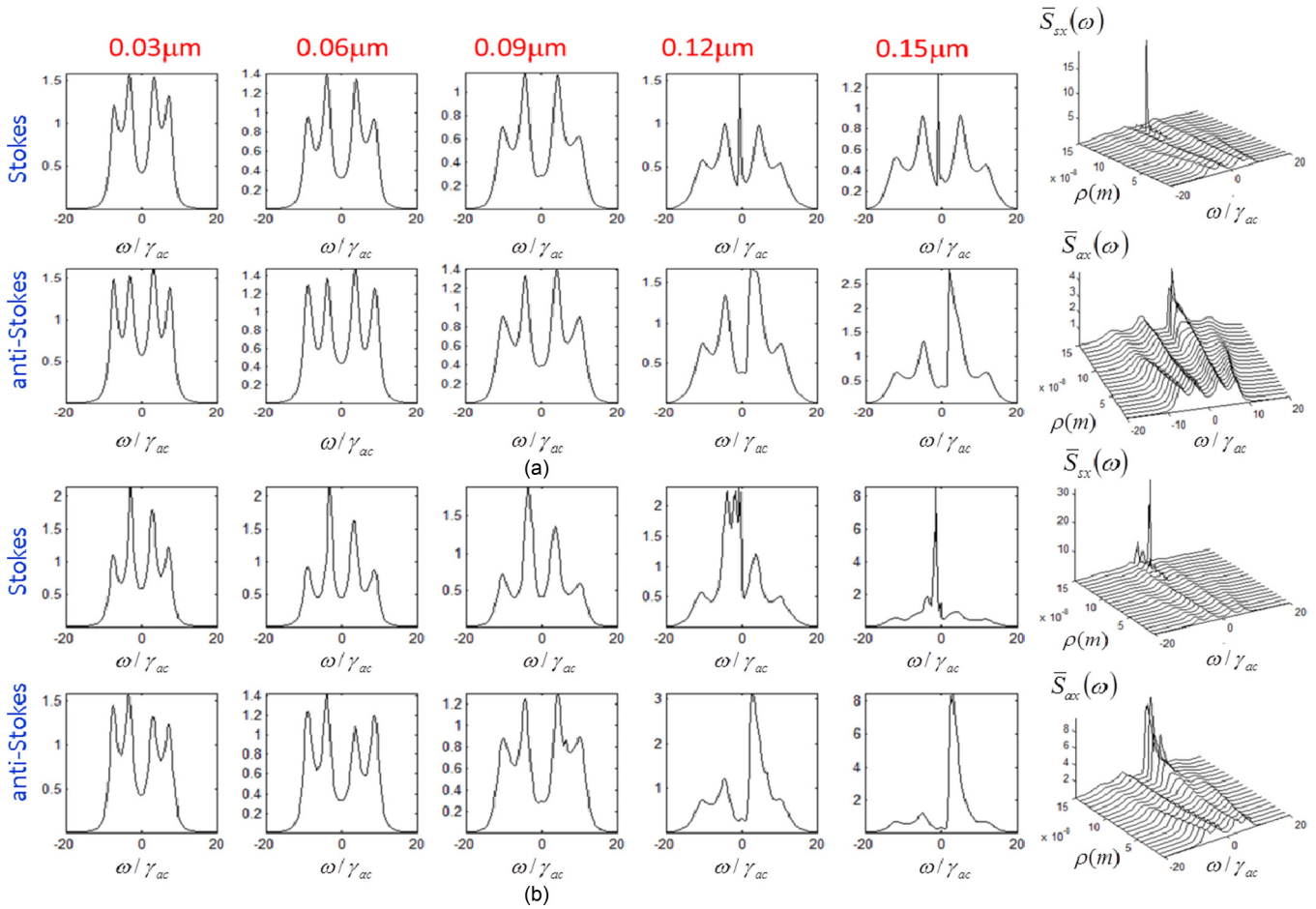

FIG. 5. (Color online) Stokes and anti-Stokes spectra with linear dispersion for different resonant fields (nonsymmetric resonant) (a) $\Omega_p = 3\gamma_{ac}$ and $\Omega_c = 7\gamma_{ac}$ and (b) $\Omega_p = 7\gamma_{ac}$ and $\Omega_c = 3\gamma_{ac}$ with several particle radii ρ indicated.

would actually yield the quantum nature of the spectra since classically there would be no distinctions between the two orderings.

Stokes vs anti-Stokes spectra. We find that the Stokes and anti-Stokes spectra look identical in the absence of dispersion (so it is trivial to show both), not only for the resonant cases [Figs. 2(a)–2(d)] but also for the Raman-electromagnetic induced transparency (EIT) [Fig. 2(e)] case when the pump and Stokes fields are far detuned and all the four transitions are off resonance as shown in Fig. 2(f). There are minor differences that are immaterial as they are not the main features.

Unexpected shift. The spectra for mesoscopic particles with finite sizes are significantly different from the spectrum of an isolated quantum particle or single atom. A closer look reveals that the side peaks in Figs. 2(b)–2(e) are shifted slightly less than $\Omega_p + \Omega_c$ from the center. This can be understood by looking at the pump-field distributions inside the particle in Fig. 3 for $|E_{px}|^2$ and $|E_{pz}|^2$. Note the presence of regions with normalized intensity $(|E_{px}|^2 + |E_{pz}|^2)/E_{po}^2$ below unity ($|E_{py}| = 0$) corresponding to an effective Rabi frequency smaller than the input value Ω_p.

Unresolved peaks. The side peaks become unresolved as the particle size ρ increases due to spectral broadening. The three (Mollow) peaks in the case of a weak field $\Omega_p = \Omega_c = \gamma_{ac}$ can no longer be resolved at around $\rho = 0.1$ μm. For larger fields $\Omega_p = \Omega_c = 10\gamma_{ac}$, the Mollow peaks are clearly visible and they can still be resolved when the particles are larger. The two side peaks for $\Omega_p \neq \Omega_c$ coalesce into a single peak and become unresolved. However, the broadening does not affect the central peak in the case $\Omega_p = \Omega_c = 10\gamma_{ac}$, which remains narrow. For different values $\Omega_p \neq \Omega_c$, there is no central peak.

Broadening mechanism. As the particle size increases, the central peak is essentially unaffected, but the side peaks undergo significant broadening and are shifted away from the center. This is due to the collective effect of spatially inhomogeneous laser fields inside the particle that causes a position-dependent ac Stark shift in the resonance frequencies. The focusing effect of the spherical particle creates a large ac Stark shift around a small spatial region. Most volumes of the spherical particle experience a range of ac Stark shift. Thus, the shift and broadening of resonance lines are due to the superpositions of a range of ac Stark shifted peaks. Note that the nature of this spectral broadening is due to a spatial factor or mesoscopic particle, an entirely different mechanism from other known broadenings, due to atomic collision, Doppler effect, or high laser fields.

Dispersion effect. When the frequency dependence of the wave vector is included through $\varepsilon_f(\omega)$ in Eq. (28), the spectra show a significant difference at a certain particle size. This is due to the presence of morphology-dependent resonant

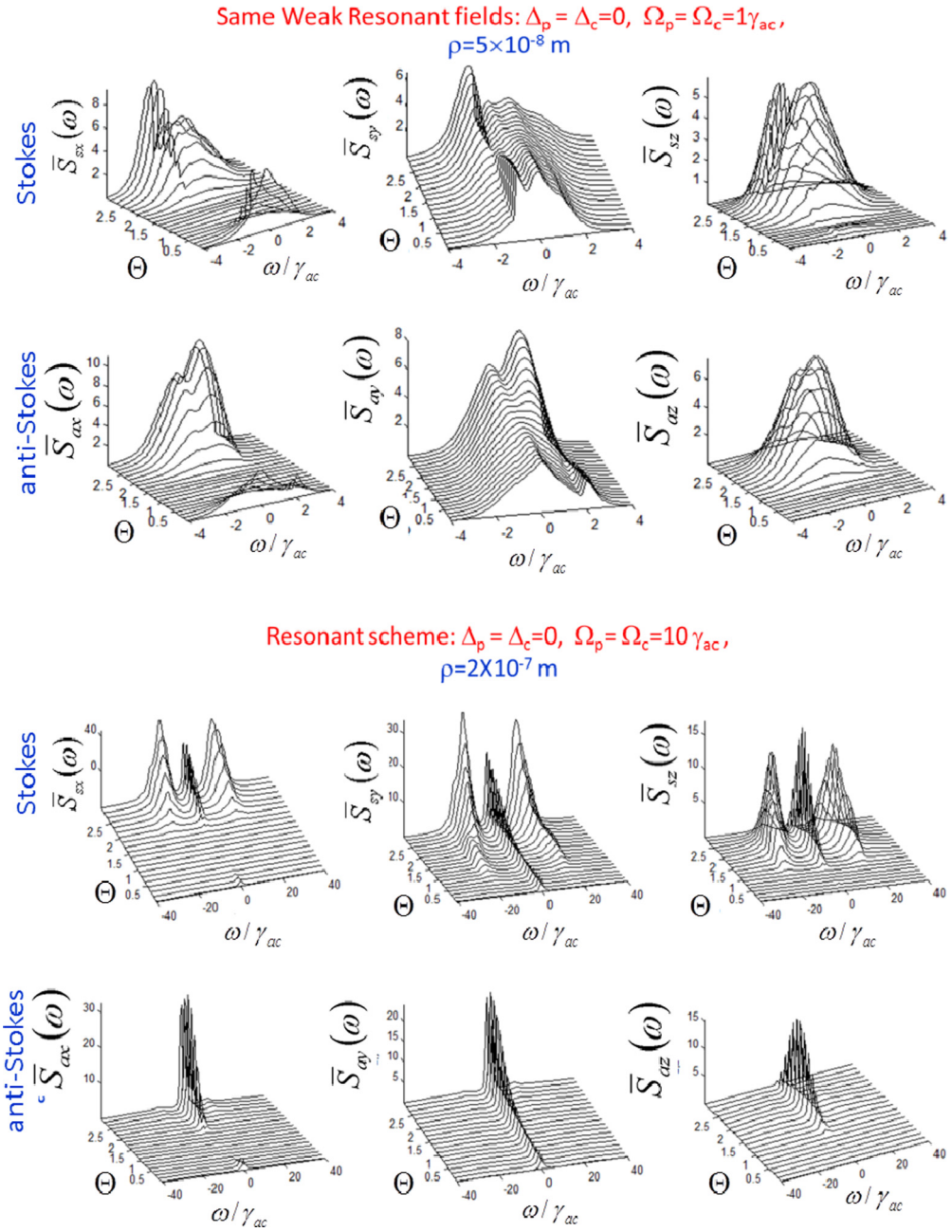

FIG. 6. (Color online) Angular-dependent Stokes and the anti-Stokes spectra with linear dispersion for the same resonant fields: (a) weak fields $\Omega_p = \Omega_c = \gamma_{ac}$ and (b) strong fields $\Omega_p = \Omega_c = 10\gamma_{ac}$.

(MDR) peaks near the center. In Fig. 4(a) for $\Omega_p = \Omega_c = \gamma_{ac}$ it can be clearly seen that the narrow MDR peak in the Stokes spectra is at around $-\gamma_{ac}$ and the slightly broader peak in the anti-Stokes spectra is at $2\gamma_{ac}$ for $\rho \simeq 0.01$ μm. For stronger fields, as shown in Fig. 4(b) with $\Omega_p = \Omega_c = 10\gamma_{ac}$, the MDR peaks are not seen until $\rho \simeq 0.1$ μm. The MDR peaks grow with the particle radius. Their positions do not change with laser parameters but remain the same. These features hold for different laser fields (nonsymmetric resonant) as shown in Fig. 5. Thus, we may say that the strong fields can reduce the effect of particle size on the spectra.

Angular dependence. In the absence of dispersion ($\varepsilon_{s,a}$ is constant) the spectra do not vary with the angle of observation Θ and field components (x,y,z), although their absolute values change. We found the variation of the spectra with the observation angle Θ through Eq. (34) and the presence of dispersive loss or gain through the terms $e^{2\,\mathrm{Im}k_s(\omega)\hat{R}\cdot\mathbf{r}}$ and $e^{2\,\mathrm{Im}k_a(\omega)\hat{R}\cdot\mathbf{r}}$ in the integrals of $S_{s,q}(\omega)$ and $S_{a,q}(\omega)$. For $\rho =$ 1 nm, the spectra do not depend on the angle, although the magnitude of the peaks changes with the angle. For $\rho = 10$ nm or larger, the spectra begin to change with Θ, as shown in Figs. 6 and 7 for nonsymmetric resonant fields and the Raman EIT scheme. The variation of the spectra with Θ can be clearly seen, especially in the case of the same weak resonant fields. Fano-like dips appear for weak symmetric resonant fields, while the side peaks of the Mollow triplet is comparable to

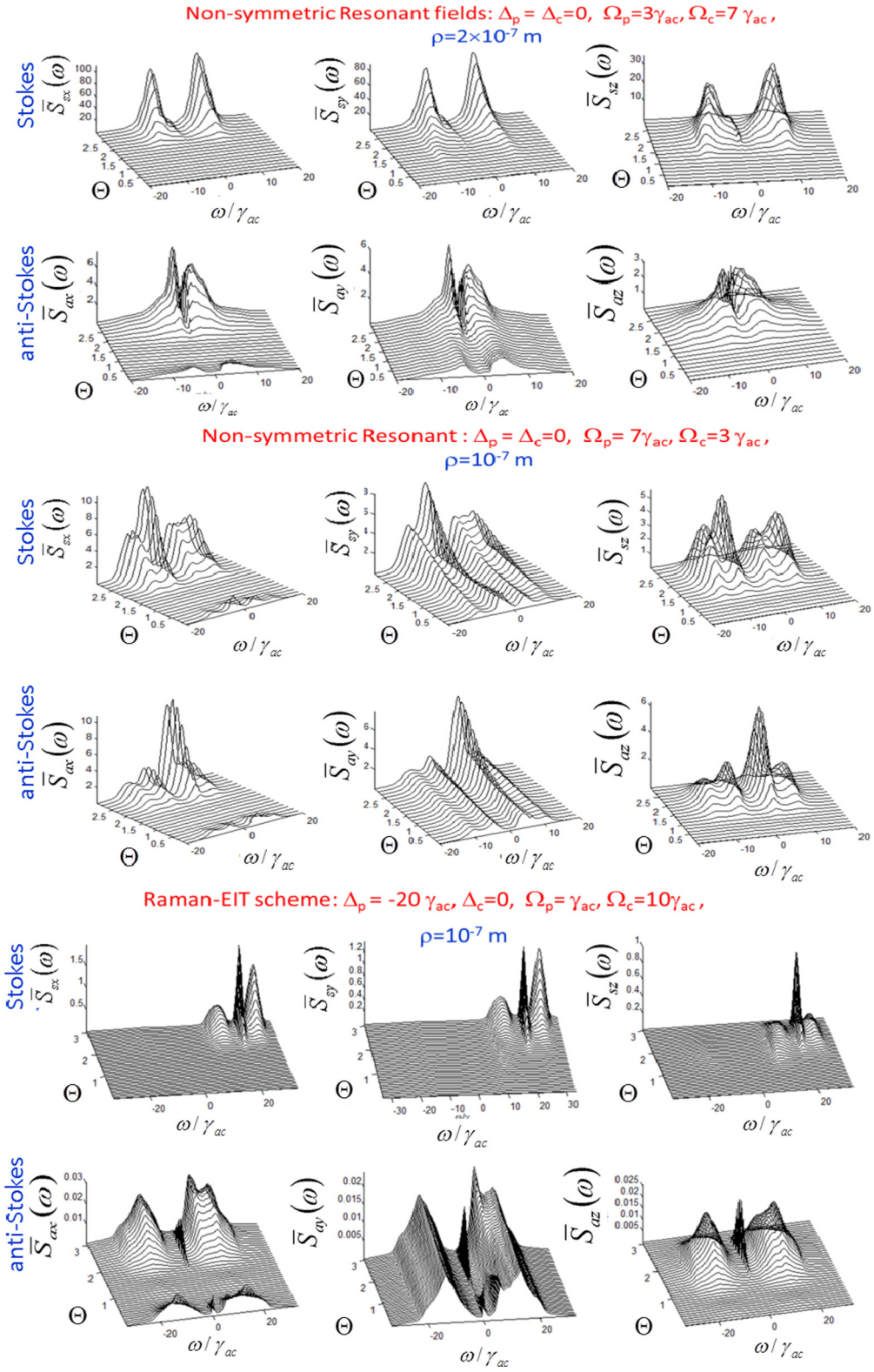

FIG. 7. (Color online) Angular-dependent Stokes and the anti-Stokes spectra with linear dispersion for nonsymmetric fields: (a) $\Omega_p = 3\gamma_{ac}$ and $\Omega_c = 7\gamma_{ac}$, (b) $\Omega_p = 7\gamma_{ac}$ and $\Omega_c = 3\gamma_{ac}$, and (c) the Raman EIT scheme $\Delta_p = -20\gamma_{ac}$, $\Delta_c = 0$, $\Omega_p = \gamma_{ac}$, and $\Omega_c = 10\gamma_{ac}$.

or higher than the central peak for high fields (in Fig. 6). For nonsymmetric resonant fields, the four peaks are not clearly shown (in Fig. 7). The Stokes peaks in the Raman EIT scheme are displaced from zero due to detuning, while the anti-Stokes spectrum has a narrow peak at certain angles. The scattered Stokes and anti-Stokes electric fields acquire the y-component fields after scattering, which has spectra similar to that of the x component but quite different from the spectra of the z component that vanishes at $\Theta = 0,\pi$ due to transversality of the waves.

In summary, the mesoscopic nature of the microparticle hides or modifies the spectral peaks originally formed due to quantum coherence and laser interaction effects. The narrow side peaks can no longer be resolved. We expect the results of this mechanism of spectral broadening to have implications on spectroscopy of mesoscopic materials composed of quantum particles.

ACKNOWLEDGMENT

This work was supported by the University of Malaya, the Ministry of Education, High Impact Research program Grant No. UM.C/625/1/HIR/MoE/CHAN/04.

APPENDIX A: POWER SPECTRUM AND FIRST-ORDER CORRELATION FUNCTION

The Fourier transform for a convolution reads $\int_{-\infty}^{\infty} e^{i\omega t}[\int_{-\infty}^{\infty} A(t')B(t-t')dt']dt = \tilde{A}(\omega)\tilde{B}(\omega)$. However, it should be realized that this expression is not readily usable here. To connect the spectrum to the correlation function $C(\tau) = \int_{-\infty}^{\infty} \tilde{E}^*(t)\tilde{E}(t+\tau)dt$, we may not use the convolution theorem directly. Instead, by definition of the Fourier transform of the electric field $\tilde{E}(\omega) = \frac{1}{\sqrt{2\pi}} \int_{-\infty}^{\infty} \tilde{E}(t)e^{i\omega t}dt$ we have

$$\begin{aligned} S(\omega) &= |\tilde{E}(\omega)|^2 = \tilde{E}^*(-\omega)\tilde{E}(\omega) \\ &= \frac{1}{2\pi}\int_{-\infty}^{\infty} e^{-i\omega t}\tilde{E}^*(t)dt \int_{-\infty}^{\infty} e^{i\omega t'}\tilde{E}(t')dt' \\ &= \frac{1}{2\pi}\int_{-\infty}^{\infty} e^{i\omega(t'-t)} \int_{-\infty}^{\infty} \tilde{E}^*(t)\tilde{E}(t')dt'dt. \end{aligned} \tag{A1}$$

Defining $\tau = t' - t$, we recover the spectrum as the Fourier transform of the correlation function

$$S(\omega) = \frac{1}{2\pi}\int_{-\infty}^{\infty} e^{i\omega\tau}C(\tau)d\tau. \tag{A2}$$

For quantum fields, the normal- and antinormal-order spectra are defined, respectively, as $S^n(\omega) = \langle \tilde{E}^\dagger(-\omega)\tilde{E}(\omega)\rangle = \frac{1}{\pi}\mathrm{Re}\int_{-\infty}^{\infty} e^{i\omega\tau}\langle \tilde{E}^\dagger(t)\tilde{E}(t+\tau)\rangle d\tau$ and $S^{an}(\omega) = \langle \tilde{E}(\omega)\tilde{E}^\dagger(-\omega)\rangle = \frac{1}{\pi}\mathrm{Re}\int_{-\infty}^{\infty} e^{i\omega\tau}\langle \tilde{E}(t+\tau)\tilde{E}^\dagger(t)\rangle d\tau$. For unpolarized detection we may also compute the spectrum due to all q components

$$S_f^n(\omega) = Re\langle \tilde{\mathbf{E}}_f^\dagger(-\omega)\cdot\tilde{\mathbf{E}}_f(\omega)\rangle = \sum_{q=x,y,z} S_{fq}^n(\omega), \tag{A3}$$

$$S_f^{an}(\omega) = Re\langle \tilde{\mathbf{E}}_f(\omega)\cdot\tilde{\mathbf{E}}_f^\dagger(-\omega)\rangle = \sum_{q=x,y,z} S_{fq}^{an}(\omega). \tag{A4}$$

The spectrum of an unpolarized signal is unaffected and remains the same as the spectrum of any polarized signal since the summation only involves the transition dipole matrix elements and the observation angles Θ,Φ through $\sum_{q=x,y,z}|\wp_{sq}^{\perp}|^2$ that are frequency independent.

APPENDIX B: DIFFUSION COEFFICIENTS

Using the 16 coupled Heisenberg-Langevin equations of motion for the atomic operators (corresponding to coherences and populations) for the double Raman scheme, we obtain the diffusion coefficients $2\tilde{D}_{j,l}^{n(an)}$ in a frequency domain, given in Eqs. (32) and (37). First, we use the Einstein relation

$$2D_{A,B} = \left\langle \frac{d(AB)}{dt} - A\left(\frac{dB}{dt} - F_b\right) - \left(\frac{dA}{dt} - F_a\right)B \right\rangle, \tag{B1}$$

where $A = \hat{\sigma}_j$ and $B = \hat{\sigma}_l$ are atomic operators, with $j,l \in 1,2,3,4$ ($1 = ac$, $2 = ad$, $3 = bc$, and $4 = bd$). Then we transform to a frequency domain and eliminate the rapid time-varying exponential.

1. Normal-order diffusion coefficients

Normal-order diffusion coefficients $2D_{j,l}^{an}$ are given here, where $j,l \in 1,2,3,4$ ($1 = ac$, $2 = ad$, $3 = bc$, and $4 = bd$). For example, $2D_{1,1}^{n}$ is evaluated as $2D_{1,1}^{n} = 2D_{ca,ac} = \frac{d}{dt}\langle\hat{\sigma}_{ca}\hat{\sigma}_{ac}\rangle - \langle\hat{\sigma}_{ca}[\frac{d}{dt}\hat{\sigma}_{ac} - \hat{F}_{ac}]\rangle - \langle[\frac{d}{dt}\hat{\sigma}_{ca} - \hat{F}_{ca}]\hat{\sigma}_{ac}\rangle$. Using a similar method, other normal-order diffusion coefficients are found. All the nonzero normal-order diffusion coefficients are

$$\begin{aligned}
2\tilde{D}_{1,1}^{n} &= 2\tilde{D}_{ca,ac} = \Gamma_{ac}\langle\hat{\sigma}_{aa}\rangle + \Gamma_{dc}\langle\hat{\sigma}_{dd}\rangle + 2\gamma_{ac}\langle\hat{\sigma}_{cc}\rangle, \\
2\tilde{D}_{1,2}^{n} &= 2\tilde{D}_{ca,ad} = (-\gamma_{dc} + \gamma_{ac} + \gamma_{ad})\langle\hat{p}_{cd}\rangle, \\
2\tilde{D}_{2,1}^{n} &= 2\tilde{D}_{da,ac} = (-\gamma_{dc} + \gamma_{ac} + \gamma_{ad})\langle\hat{p}_{dc}\rangle, \\
2\tilde{D}_{2,2}^{n} &= 2\tilde{D}_{da.ad} = [2\gamma_{ad} - (\Gamma_{db} + \Gamma_{dc})]\langle\hat{\sigma}_{dd}\rangle, \\
2\tilde{D}_{3,3}^{n} &= 2\tilde{D}_{cb,bc} = \Gamma_{ac}\langle\hat{\sigma}_{aa}\rangle + \Gamma_{dc}\langle\hat{\sigma}_{dd}\rangle + 2\gamma_{bc}\langle\hat{\sigma}_{cc}\rangle, \\
2\tilde{D}_{3,4}^{n} &= 2\tilde{D}_{cb,bd} = (-\gamma_{dc} + \gamma_{bc} + \gamma_{db})\langle\hat{p}_{cd}\rangle, \\
2\tilde{D}_{4,3}^{n} &= 2\tilde{D}_{db,bc} = (-\gamma_{dc} + \gamma_{bc} + \gamma_{db})\langle\hat{p}_{dc}\rangle, \\
2\tilde{D}_{4,4}^{n} &= 2\tilde{D}_{db,bd} = [2\gamma_{db} - (\Gamma_{db} + \Gamma_{dc})]\langle\hat{\sigma}_{dd}\rangle.
\end{aligned} \tag{B2}$$

2. Antinormal-order diffusion coefficients

In a similar manner, the antinormal-order diffusion coefficients $2D_{j,l}^{an}$ with nonzero values are obtained

$$\begin{aligned}
2\tilde{D}_{1,1}^{an} &= 2\tilde{D}_{ac,ca} = [-(\Gamma_{ab} + \Gamma_{ac}) + 2\gamma_{ac}]\langle\hat{\sigma}_{aa}\rangle, \\
2\tilde{D}_{1,3}^{an} &= 2\tilde{D}_{ac,cb} = (-\gamma_{ab} + \gamma_{bc} + \gamma_{ac})\langle\hat{p}_{ab}\rangle, \\
2\tilde{D}_{2,2}^{an} &= 2\tilde{D}_{ad.da} = [-(\Gamma_{ab} + \Gamma_{ac}) + 2\gamma_{ad}]\langle\hat{\sigma}_{aa}\rangle, \\
2\tilde{D}_{2,4}^{an} &= 2\tilde{D}_{ad,db} = (-\gamma_{ab} + \gamma_{db} + \gamma_{ad})\langle\hat{p}_{ab}\rangle, \\
2\tilde{D}_{3,1}^{an} &= 2\tilde{D}_{bc,ca} = (-\gamma_{ab} + \gamma_{ac} + \gamma_{bc})\langle\hat{p}_{ba}\rangle, \\
2\tilde{D}_{3,3}^{an} &= 2\tilde{D}_{bc,cb} = \Gamma_{ab}\langle\hat{\sigma}_{aa}\rangle + \Gamma_{db}\langle\hat{\sigma}_{dd}\rangle + 2\gamma_{bc}\langle\hat{\sigma}_{bb}\rangle, \\
2\tilde{D}_{4,2}^{an} &= 2\tilde{D}_{bd,da} = (-\gamma_{ab} + \gamma_{ad} + \gamma_{db})\langle\hat{p}_{ba}\rangle, \\
2\tilde{D}_{4,4}^{an} &= 2\tilde{D}_{bd,db} = \Gamma_{ab}\langle\hat{\sigma}_{aa}\rangle + \Gamma_{db}\langle\hat{\sigma}_{dd}\rangle + 2\gamma_{db}\langle\hat{\sigma}_{bb}\rangle,
\end{aligned} \tag{B3}$$

where Γ_x is the spontaneous emission rate and γ_x the decoherence rate, with $x = ac,ab,db,dc$.

APPENDIX C: MATRIX ELEMENTS IN DIFFUSION COEFFICIENTS

In order to compute the diffusion coefficients we have to solve the following coupled equations for the populations.

Taking the Fourier transform, we have the equations for populations in the frequency domain

$$0 = i(\Omega_c \hat{p}_{ab} - \Omega_c^* \hat{p}_{ba}) - T_{aa}(\omega)\hat{\sigma}_{aa} + \Gamma_{ab}\bar{n}_{ab}\hat{\sigma}_{bb} + \Gamma_{ac}\bar{n}_{ac}\hat{\sigma}_{cc} + \hat{F}_{aa}, \quad \text{(C1)}$$

$$0 = i(\Omega_c^* \hat{p}_{ba} - \Omega_c \hat{p}_{ab}) - T_{bb}(\omega)\hat{\sigma}_{bb} + \Gamma_{ab}(\bar{n}_{ab}+1)\hat{\sigma}_{aa} + \Gamma_{db}(\bar{n}_{db}+1)\hat{\sigma}_{dd} + \hat{F}_{bb}, \quad \text{(C2)}$$

$$0 = i(\Omega_p^* \hat{p}_{cd} - \Omega_p \hat{p}_{dc}) - T_{cc}(\omega)\hat{\sigma}_{cc} + \Gamma_{ac}(\bar{n}_{ac}+1)\hat{\sigma}_{aa} + \Gamma_{dc}(\bar{n}_{dc}+1)\hat{\sigma}_{dd} + \hat{F}_{cc}, \quad \text{(C3)}$$

$$0 = i(\Omega_p \hat{p}_{dc} - \Omega_p^* \hat{p}_{cd}) - T_{dd}(\omega)\hat{\sigma}_{dd} + \Gamma_{db}\bar{n}_{db}\hat{\sigma}_{bb} + \Gamma_{dc}\bar{n}_{dc}\hat{\sigma}_{cc} + \hat{F}_{dd}, \quad \text{(C4)}$$

where $\hat{p}_{ab}(z,\omega) = e^{-i\nu_q t}\hat{\sigma}_{ab}$ and $\hat{p}_{dc}(z,\omega) = e^{-i\nu_p t}\hat{\sigma}_{dc}$, with Γ_x and γ_x ($x = ac, ab, db, dc$) defined in Appendix B, and $\bar{n}_x = [\exp(\theta_x) - 1]^{-1}$ represents the thermal photon numbers $\theta_x = \hbar\omega_x / k_B T$,

$$\begin{aligned} T_{aa}(\omega) &= \Gamma_{ab}(\bar{n}_{ab}+1) + \Gamma_{ac}(\bar{n}_{ac}+1) - i\omega, \\ T_{bb}(\omega) &= \Gamma_{ab}\bar{n}_{ab} + \Gamma_{db}\bar{n}_{db} - i\omega, \\ T_{cc}(\omega) &= \Gamma_{ac}\bar{n}_{ac} + \Gamma_{dc}\bar{n}_{dc} - i\omega, \\ T_{dd}(\omega) &= \Gamma_{db}(\bar{n}_{db}+1) + \Gamma_{dc}(\bar{n}_{dc}+1) - i\omega. \end{aligned} \quad \text{(C5)}$$

Note that these equations for the populations are decoupled from Eqs. (1)–(4) for $\hat{p}_{ac}(z,\omega)$, $\hat{p}_{ad}(z,\omega)$, $\hat{p}_{bc}(z,\omega)$, and $\hat{p}_{bd}(z,\omega)$. The equations for coherences at laser transitions are

$$\hat{p}_{ab}(\omega) = \frac{-i\Omega_c^*(\hat{\sigma}_{bb} - \hat{\sigma}_{aa}) + \hat{F}_{ab}e^{-i\nu_q t}}{T_{ab}(\omega)}, \quad \text{(C6)}$$

$$\hat{p}_{dc}(\omega) = \frac{-i\Omega_p^*(\hat{\sigma}_{cc} - \hat{\sigma}_{dd}) + \hat{F}_{dc}e^{-i\nu_p t}}{T_{dc}(\omega)}, \quad \text{(C7)}$$

where $T_{ab}(\omega) = i\Delta_{ab} + \gamma_{ab} - i\omega$ and $T_{dc}(\omega) = i\Delta_{dc} + \gamma_{dc} - i\omega$. Since $\hat{p}_{jk}(-\omega) = [\hat{p}_{kj}(\omega)]^\dagger$, actually

$$\hat{p}_{ba}(-\omega) = [\hat{p}_{ab}(\omega)]^\dagger = \frac{i\Omega_c(\hat{\sigma}_{bb} - \hat{\sigma}_{aa}) + \hat{F}_{ab}^\dagger e^{i\nu_q t}}{-i\Delta_{ab} + \gamma_{ab} + i\omega} = \frac{i\Omega_c(\hat{\sigma}_{bb} - \hat{\sigma}_{aa}) + \hat{F}_{ab}^\dagger e^{i\nu_q t}}{T_{ab}^*(\omega)}$$

and not $\hat{p}_{ba}(\omega)$. Eliminating $\hat{p}_{ab}$ and $\hat{p}_{dc}$ in Eqs. (C1)–(C4) and using $I - \hat{\sigma}_{aa} - \hat{\sigma}_{bb} - \hat{\sigma}_{cc} = \hat{\sigma}_{dd}$, we have the solutions needed in the diffusion coefficients

$$\begin{aligned} \langle \hat{p}_{aa} \rangle &= \frac{1}{D}(N_2 N_{1b} N_{3c} + N_3 N_{1c} N_{2b}), \\ \langle \hat{p}_{bb} \rangle &= \frac{1}{D}(N_{1a} N_2 N_{3c} - N_{3a} N_{1c} N_2 + N_{2a} N_{1c} N_3), \\ \langle \hat{p}_{cc} \rangle &= \frac{1}{D}(N_{3a} N_{1b} N_2 + N_{1a} N_{2b} N_3 - N_{2a} N_{1b} N_3), \end{aligned} \quad \text{(C8)}$$

where

$$D = N_{1a}N_{2b}N_{3c} + N_{1a}N_{2b}N_3 + N_{1a}N_2N_{3c} + N_{2a}N_{1c}N_3 + N_2N_{1b}N_{3c} + N_{3a}N_{1b}N_2 + N_3N_{1c}N_{2b} - N_{2a}N_{1b}N_{3c} - N_{2a}N_{1b}N_3 - N_{3a}N_{1c}N_{2b} - N_{3a}N_{1c}N_2; \quad \text{(C9)}$$

$$\begin{aligned} N_{1a} &= \delta_c + T_{aa}(\omega), \\ N_{1b} &= \delta_c + \Gamma_{ab}\bar{n}_{ab}, \\ N_{1c} &= \Gamma_{ac}\bar{n}_{ac}; \end{aligned} \quad \text{(C10)}$$

$$\begin{aligned} N_{2a} &= \delta_c + \Gamma_{ab}(\bar{n}_{ab}+1), \\ N_{2b} &= \delta_c + T_{bb}(\omega), \\ N_2 &= \Gamma_{db}(\bar{n}_{db}+1); \end{aligned} \quad \text{(C11)}$$

$$\begin{aligned} N_{3a} &= \Gamma_{ac}(\bar{n}_{ac}+1), \\ N_{3c} &= \delta_p + T_{cc}(\omega), \\ N_3 &= \delta_p + \Gamma_{dc}(\bar{n}_{dc}+1), \end{aligned} \quad \text{(C12)}$$

with the power broadenings $\delta_c = \frac{|\Omega_c|^2}{T_{ab}(\omega)} + \frac{|\Omega_c|^2}{T_{ab}^*(\omega)}$ and $\delta_p = \frac{|\Omega_p|^2}{T_{dc}^*(\omega)} + \frac{|\Omega_p|^2}{T_{dc}(\omega)}$.

[1] M. O. Scully and C. H. R. Ooi, J. Opt. B **6**, S816 (2004).
[2] A. K. Patnaik, G. S. Agarwal, C. H. R. Ooi, and M. O. Scully, Phys. Rev. A **72**, 043811 (2005).
[3] C. H. R. Ooi, Phys. Rev. A **75**, 043817 (2007); C. H. Raymond Ooi, B.-G. Kim, and H.-W. Lee, *ibid.* **75**, 063801 (2007).
[4] C. H. Raymond Ooi and B. L. Lan, Phys. Rev. A **81**, 063832 (2010).
[5] C. H. R. Ooi, Phys. Rev. A **76**, 013809 (2007); C. Benkert *et al.*, *ibid.* **41**, 2756 (1990).
[6] C. H. R. Ooi, Q. Q. Sun, M. S. Zubairy, and M. O. Scully, Phys. Rev. A **75**, 013820 (2007).
[7] C. H. Bennett and P. W. Shor, IEEE Trans. Inf. Theory **44**, 2724 (1998).
[8] D. E. Chang, V. Vuletic, and M. D. Lukin, Nat. Photon. **8**, 685 (2014); M. Gullans, D. E. Chang, F. H. L. Koppens, F. J. García de Abajo, and M. D. Lukin, Phys. Rev. Lett. **111**, 247401 (2013).
[9] F. Javier García de Abajo, Nature (London) **483**, 417 (2012).
[10] C. H. R. Ooi, G. Beadie, G. W. Kattawar, J. F. Reintjes, Y. Rostovtsev, M. S. Zubairy, and M. O. Scully, Phys. Rev. A **72**, 023807 (2005).
[11] K. M. Leung, Phys. Rev. A **33**, 2461 (1986).
[12] G. Kurizki and A. Nitzan, Phys. Rev. A **38**, 267 (1988).
[13] S. Das and J. I. Gersten, Phys. Rev. B **37**, 6063 (1988).
[14] M. Montagna and R. Dusi, Phys. Rev. B **52**, 10080 (1995).
[15] Y. Pavlyukh and W. Hübner, Phys. Rev. B **70**, 245434 (2004).
[16] M. Sargent III, M. O. Scully, and W. E. Lamb, Jr., *Laser Physics* (Addison-Wesley, London, 1974).

[17] C. H. R. Ooi and M. S. Zubairy, Phys. Rev. A **75**, 053822 (2007); C. H. R. Ooi and M. O. Scully, *ibid.* **76**, 043822 (2007).
[18] R. R. Puri, *Mathematical Methods of Quantum Optics* (Springer, Berlin, 2001).
[19] R. J. Glauber, Phys. Rev. **130**, 2529 (1963).
[20] L. Mandel, Phys. Rev. **152**, 438 (1966).
[21] C. F. Bohren and D. R. Huffman, *Absorption and Scattering of Light by Small Particles* (Wiley, New York, 1983).
[22] C. H. R. Ooi, J. Raman Spectrosc. **40**, 714 (2009).